Journal of Alloys and Compounds 489 (2010) 620–625

Contents lists available at ScienceDirect

Journal of Alloys and Compounds

journal homepage: www.elsevier.com/locate/jallcom

A ternary linear compound T_2 and its phase equilibrium relationships in Mg–Zn–Nd system at 400 °C

M.L. Huang[a,b], H.X. Li[b,*], H. Ding[b], Z.Y. Tang[b], R.B. Mei[a,b], H.T. Zhou[a,b], R.P. Ren[b], S.M. Hao[b]

[a] *Department of Materials Science and Engineering, Northeastern University at Qinhuangdao, 066004, China*
[b] *School of Materials and Metallurgy, Northeastern University, Shenyang, Liaoning 110004, China*

ARTICLE INFO

Article history:
Received 14 May 2009
Received in revised form
18 September 2009
Accepted 22 September 2009
Available online 30 September 2009

Keywords:
Mg–Zn–Nd system
Ternary linear compound
T_2 phase
Crystal structure
Phase equilibrium

ABSTRACT

The composition and the crystal structure of the phases in the alloys of Mg–Zn–Nd system at 400 °C have been studied by scanning electron microscopy (SEM), electron probe microanalysis (EPMA), X-ray diffraction (XRD) and selected area electron diffraction (SAED) of transmission electron microscopy (TEM). The phase equilibrium relationships have been identified. As a result, a linear ternary compound T_2 phase has been identified. The general chemical formula of T_2 phase is $(Mg, Zn)_{11.5}Nd$ and the crystal structure of that is C-centered orthorhombic. As the results, the other three ternary compounds T_1 phase, T_3 phase and T_4 phase have also been identified. The partial isothermal section of phase diagram of Mg–Zn–Nd system at 400 °C has been established.

1. Introduction

Magnesium alloys are one of the lightest structural materials, and whose applications potential in automobile industry, aviation industry and electron industry have been focused in recent years [1–3]. Compared to applications of iron-based alloys and aluminum alloys, the applications of magnesium alloys are limited because of their poor plasticity at room temperature and their poor mechanical properties at elevated temperatures. Therefore, developing magnesium alloys with improved mechanical properties especially at elevated temperatures is crucial for their applications. The addition of rare earth elements can improve the mechanical properties of magnesium alloys especially at elevated temperatures. In recent years the magnesium alloys with the addition of rare earth elements are studied widely [4–8].

Mg–Zn system is a basic system for Mg alloys. But in this system, there is a low eutectic temperature. For this reason, the mechanical properties of Mg–Zn alloys are poor at elevated temperatures. The addition of rare earth element can not only refine the grains of the Mg–Zn system alloys [9–18], but also improve the creep resistance at elevated temperatures, because of the formation of the high melting-point compounds.

Though the mechanical properties [19–21] and the quasicrystal phase [22,23] of some alloys in Mg–Zn–Nd system have been studied in recent years, the information is still not sufficient for alloy design. It is well known that alloy phase diagram is the guide for alloy design. However the equilibrium phase diagram of the Mg–Zn–Nd system has not been studied in detail even in the Mg-rich corner. The isothermal sections of Mg–Zn–Nd system at 400 °C and 500 °C have been only reported by Drits et al. [24]. Only two three-phase regions have been reported at 400 °C, and one three-phase region has been reported at 500 °C. The isothermal sections containing relatively more phase regions near 300 °C have been reported by Drits et al. and Kinzhibalo et al. [25], but the results of the two groups are conflicting to each other. The compounds identified by Drits et al. in Mg-rich corner at 297 °C were $Mg_{12}Nd$, Mg_6NdZn_3, Mg_4NdZn_5, Mg_7NdZn_{12} and $Mg_{51}Zn_{20}$. And those identified by Kinzhibalo et al. in Mg-rich corner at 300 °C were $Mg_{12}Nd$, $MgNd_4Zn_5$, $Mg_6Nd_2Zn_7$, $Mg_2Nd_2Zn_9$ and MgZn. The ternary compounds reported by these two groups were totally different at nearly the same temperature, and the phase relationships were also different as shown in Fig. 1 [26]. So it is necessary to have a systematic study for the phase diagram of the Mg–Zn–Nd system in the Mg-rich corner.

This paper is one part of the research on the phase equilibrium of Mg–Zn–Nd system. In order to obtain exact information for Mg-based alloy design, the ternary compounds in the low-Nd side of Mg–Zn–Nd system and their phase equilibrium at 400 °C were studied.

---

[*] Corresponding author. Tel.: +86 24 83687746; fax: +86 24 83686455.
E-mail addresses: mingli_huang@126.com, hxli@mail.neu.edu.cn (H.X. Li).

0925-8388/$ – see front matter © 2009 Elsevier B.V. All rights reserved.
doi:10.1016/j.jallcom.2009.09.131

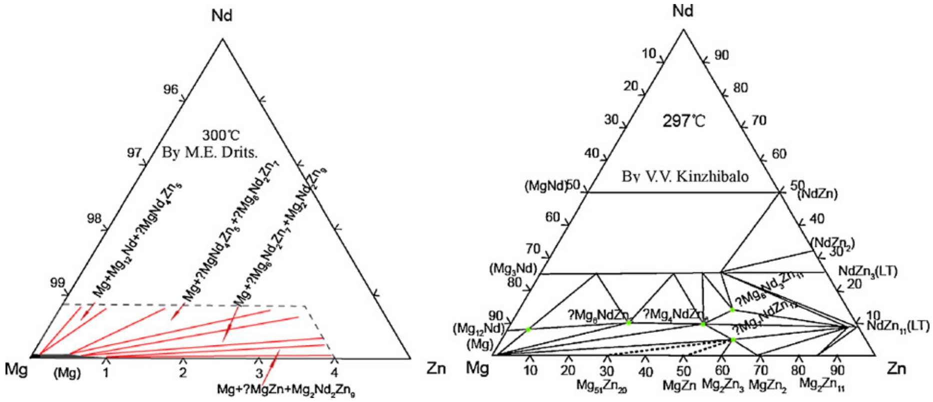

Fig. 1. Isothermal sections of Mg–Zn–Nd system reported in literatures.

2. Experimental procedures

Seven alloys with different compositions in the low-Nd side of the Mg–Zn–Nd ternary system were prepared in this work, and the weight of each alloy was 30 g. The purity of Mg and Zn was 99.99 wt%, and the purity of Nd was about 99.8 wt%. Because of the serious loss of Mg during melting, the content of Mg was added 10 wt% more than its theoretical content. The pure metals were mixed up together, and then melting back in the carbon crucible in a vacuum induction furnace under Ar atmosphere. The as-cast samples were wrapped with tantalum foils and sealed in a quartz tube with the vacuum degree of 10^{-2} Pa. The samples were equilibrium-treated at 400 °C for 504 h and then ice water-quenched.

The microstructure of each alloy was examined by scanning electron microscopy (SEM) using SSX-500 microscope. The composition of each phase in the alloys was studied by EPMA-1600 electron probe microanalyzer with a beam size of 1 μm and a voltage of 15 kV. The high pure Mg, Zn, and Nd were served as the standards to revise the characteristic radiations with ZAF4 correction. The crystal structures of phases were studied by X-ray diffraction (XRD) and transmission electron microscopy (TEM) using Siemens D5000 with Cu Kα radiation and TecnaiG^{2}20 respectively. Thin foil specimens for TEM were prepared by electronic ion polishing.

3. Results and discussion

Within the seven alloys prepared in this work, there are two alloys in two-phase equilibrium and five alloys in three-phase equilibrium. The compositions of phases (atom fraction, the same as follows) in the alloys are shown in Table 1.

3.1. The two-phase equilibrium of Mg + T_2

The equilibrium microstructures of the $Mg_{75}Zn_{20}Nd_5$ alloy and $Mg_{70}Zn_{25}Nd_5$ alloy at 400 °C are shown in Fig. 2. The black is Mg solid solution with the composition of 98.8% Mg, 1.2% Zn and ignored Nd. The grey is a ternary compound with the composition of 61.1% Mg, 31.1% Zn and 7.8% Nd, and this phase is called T_2 phase here.

The crystal structure of T_2 phase in $Mg_{75}Zn_{20}Nd_5$ alloy has been analyzed by selected area electron diffraction (SAED) of TEM. The SAED pattern of [1 0 1] zone axis of T_2 phase is shown in Fig. 3a, which suggests that T_2 phase has a C-centered orthorhombic crystal structure with the lattice parameters of $a = 0.98$ nm, $b = 1.13$ nm, and $c = 0.96$ nm. The X-ray diffraction pattern of $Mg_{75}Zn_{20}Nd_5$ alloy is shown in Fig. 3b. The diffraction peaks of Mg can be indexed, and all the other diffraction peaks can be indexed with the C-centered orthorhombic crystal structure with the parameters obtained from Fig. 3a. This suggests again that the crystal structure of T_2 phase is C-centered orthorhombic.

The results above reveal that the $Mg_{75}Zn_{20}Nd_5$ alloy is in the two-phase region of Mg + T_2 at 400 °C.

According to the microstructure of the $Mg_{75}Zn_{20}Nd_5$ alloy (Fig. 2a), the solidifying process could be deduced. During cooling, the Mg solid solution solidified from liquid first, then, with the temperature decreasing further, the eutectic reaction of $L \rightarrow (Mg) + T_2$ can be deduced to occur over 400 °C. So the microstructure of $Mg_{75}Zn_{20}Nd_5$ alloy at 400 °C was contained by Mg solid solution and the eutectic structure of E1 (Mg + T_2).

The black in $Mg_{70}Zn_{25}Nd_5$ alloy (Fig. 2b) is Mg solid solution with the composition of 96.8% Mg, 3.2% Zn and ignored Nd. The grey is a ternary compound with the composition of 53.3% Mg, 38.9% Zn and 7.8% Nd, and the Nd content of which is nearly the same as that of T_2 phase.

The diffraction peaks of $Mg_{70}Zn_{25}Nd_5$ alloy are corresponding one-to-one with those of $Mg_{75}Zn_{20}Nd_5$ alloy as shown in Fig. 3b. The diffraction peaks of Mg solid solution in the two alloys are at the same angles, but the rest of $Mg_{70}Zn_{25}Nd_5$ alloy shift to a relatively higher 2θ value regularly compared to those corresponding peaks of $Mg_{75}Zn_{20}Nd_5$ alloy. All the rest peaks of $Mg_{70}Zn_{25}Nd_5$ alloy can also be indexed with C-centered orthorhombic crystal structure with the lattice parameters of $a = 0.97$ nm, $b = 1.12$ nm, and $c = 0.95$ nm. The results of the composition and the crystal structure of the ternary compounds in the two alloys suggest that they belong to the same one ternary linear compound T_2. That is to say, T_2 phase has a C-centered orthorhombic crystal structure, and it has a continuous composition change. The chemical formula of T_2 is $(Mg, Zn)_{11.5}Nd$. The results suggest that the $Mg_{70}Zn_{25}Nd_5$ alloy is also in the two-phase region of Mg + T_2 at 400 °C.

Table 1
The compositions of phases in alloys at 400 °C (at.%).

Alloys and nominal composition	(Mg)			T_1			T_2 (linear compound)			T_3 (linear compound)			T_4			Liquid		
	Mg	Zn	Nd	Mg	Zn	Nd	Mg	Zn	Nd	Mg	Zn	Nd	Mg	Zn	Nd	Mg	Zn	Nd
$Mg_{75}Zn_{17}Nd_8$	99.0	1.0	0.0	–			**65.2**	**26.9**	**7.9**	**31.9**	**43.1**	**25.0**	–			–		
$Mg_{75}Zn_{20}Nd_5$	98.8	1.2	0.0	–			**61.1**	**31.1**	**7.8**	–			–			–		
$Mg_{51}Zn_{38}Nd_{11}$	–			–			**60.1**	–	**8.1**	**26.6**	**48.4**	**25.0**	25.2	59.1	15.7	–		
$Mg_{50}Zn_{40}Nd_{10}$	–			–			**58.6**	–	**7.9**	**26.0**	**49.0**	**25.0**	25.6	58.4	16.0	–		
$Mg_{70}Zn_{25}Nd_5$	98.9	1.1	0.0	–			**53.3**	**38.9**	**7.8**	–			–			–		
$Mg_{70}Zn_{26}Nd_4$	98.8	1.2	0.0	29.9	63.0	7.1	**50.9**	–	–	–			–			–		
$Mg_{70}Zn_{28}Nd_2$	98.8	1.2	0.0	30.0	63.0	7.0	–			–			–			70.0	30.0	0

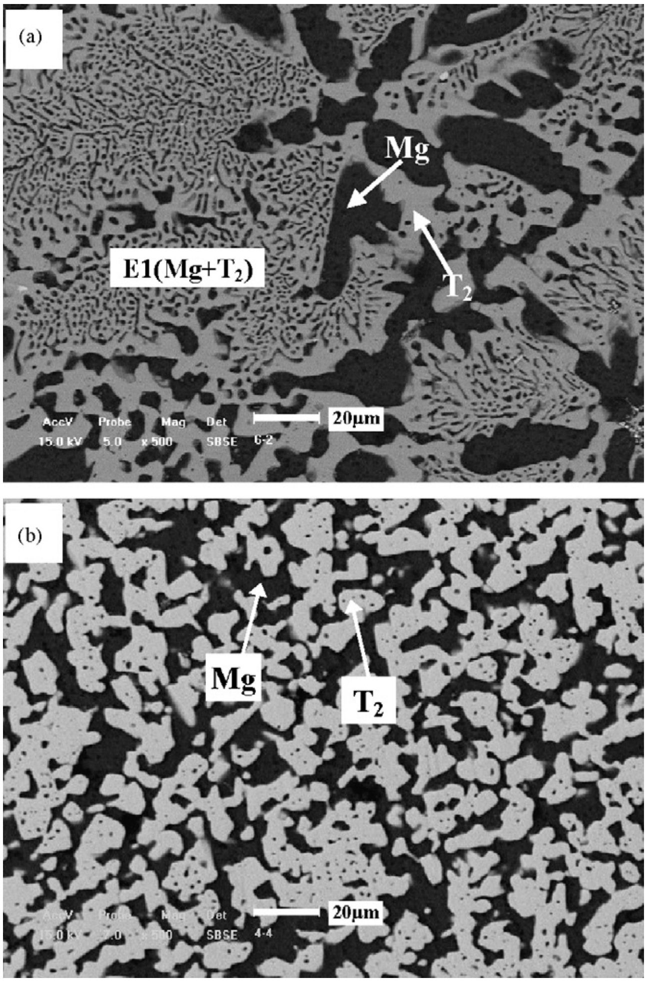

Fig. 2. Microstructures of Mg + T_2 two-phase equilibrium alloys at 400 °C. (a) $Mg_{75}Zn_{20}Nd_5$ and (b) $Mg_{70}Zn_{25}Nd_5$.

The reason why the 2θ value of peaks for the same $(h\,k\,l)$ triplet shifts to a higher angles with the increase of Zn content in T_2 phase is given here. It is well known that the radius of Zn is 0.153 nm, which is 0.019 nm shorter than that of Mg. So, when the content of Nd is not changed, the lattice parameters of T_2 should decrease with Mg content being substituted by Zn content. According to the formula of Bragg and the interplanar distance of the orthorhombic system, the formula of $2\theta = 2\arcsin(\lambda/2)\sqrt{(h^2/a^2)+(k^2/b^2)+(l^2/c^2)}$ can be obtained. The formula shows that, for each $(h\,k\,l)$ triplet, the 2θ value shifts to a higher angle with the parameters decreasing. The analysis shows that the increase of 2θ value with the increase of Zn content is reasonable.

3.2. The three-phase equilibrium of $T_2 + T_3 + Mg$

Fig. 4 is the equilibrium microstructure of $Mg_{75}Zn_{17}Nd_8$ alloy at 400 °C. The composition of the black is 99% Mg, 1% Zn and ignored Nd, which can be identified as Mg solid solution by corresponding X-ray diffraction (Fig. 5); the composition of the grey is 65.2% Mg, 26.9% Zn and 7.9% Nd, the content of Nd is nearly the same as that of T_2 phase. And the diffraction peaks of C-centered orthorhombic crystal structure with the lattice parameters of a = 0.984 nm, b = 1.135 nm, and c = 0.963 nm can be indexed from the X-ray diffraction pattern in Fig. 5. This suggests that the grey in Fig. 4 is T_2 phase. The white is called T_3 phase here, with the composition of 31.9% Mg, 43.1% Zn and 25% Nd.

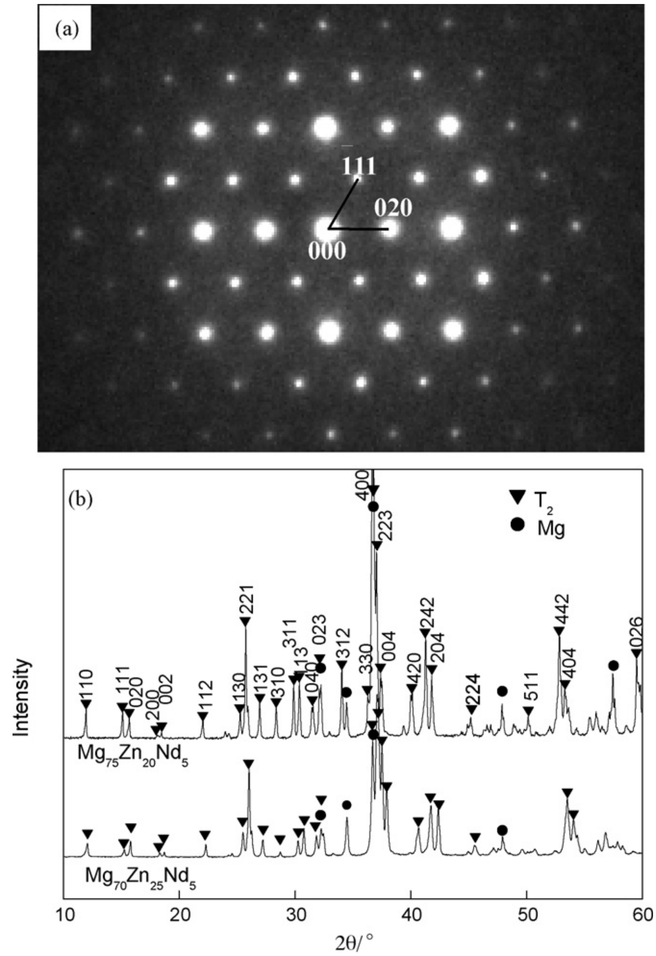

Fig. 3. SAED pattern of T_2 phase with [1 0 1] zone axis in $Mg_{75}Zn_{20}Nd_5$ alloy (a) and X-ray diffraction patterns of $Mg_{75}Zn_{20}Nd_5$ alloy and $Mg_{70}Zn_{25}Nd_5$ alloy (b) at 400 °C.

There are two types of eutectic microstructure in Fig. 4, which are E1 (T_2 + Mg) and E2 (T_3 + Mg), and E2 is surrounded by E1. It means that the formation of E2 is earlier than that of E1. And the dendritic microstructure of T_3 phase in Fig. 4 has been verified that T_3 is the pre-formation phase during solidification from liquid.

The result of Fig. 6 shows that the crystal structure of T_3 phase is the face-centered cubic. Fig. 6a and b are the SAED patterns of [1 1 0] and [1 1 1] zone axis respectively. The result of Fig. 6 shows that the lattice parameters of T_3 phase are $a = b = c$ = 0.68 nm. The diffraction peaks of T_3 phase can also be indexed from the X-ray diffraction pattern of $Mg_{75}Zn_{17}Nd_8$ alloy in Fig. 5. According to the composition in Table 1, T_3 phase is also a linear compound and the chemical formula of T_3 is $(Mg, Zn)_3Nd$.

The results obtained above suggest that $Mg_{75}Zn_{17}Nd_8$ alloy is in the three-phase region of (Mg) + T_2 + T_3 at 400 °C.

3.3. The three-phase equilibriums of Mg + Liquid (L) + T_1 and $T_2 + T_1$ + Mg

Fig. 7a is the equilibrium microstructure of alloy $Mg_{70}Zn_{28}Nd_2$ at 400 °C. The black is Mg solid solution with the composition of 98.8% Mg, 1.2% Zn and ignored Nd. The grey is indicated in liquid state at 400 °C, though the composition of which is 70% Mg, 30% Zn, and free of Nd. The composition and microstructure of L at 400 °C can be kept to room temperature by quick cooling. The composition of the white is 29.9% Mg, 63% Zn and 7.1% Nd, which is the same as that of the T_1 phase with hexagonal crystal structure with the lattice parameters of $a = b$ = 1.47 nm, and c = 0.87 nm [27]. The peaks of T_1

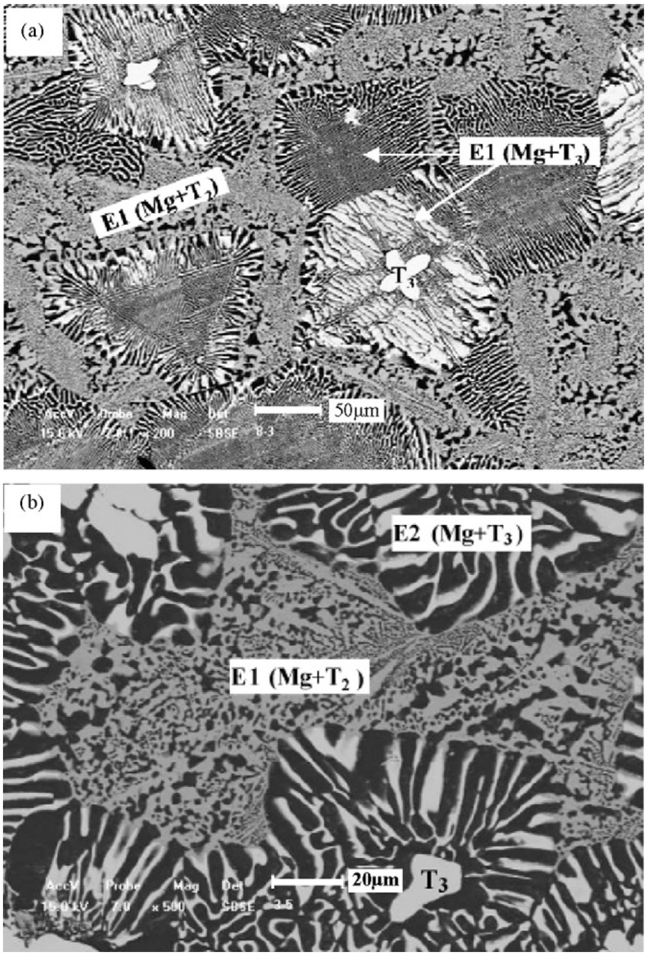

Fig. 4. Microstructures of $Mg_{75}Zn_{17}Nd_8$ alloy at 400 °C. (a) At lower magnification and (b) at higher magnification.

phase and Mg solid solution could be indexed in the corresponding X-ray diffraction pattern (Fig. 7b). So the white ternary compound in Fig. 7a must be T_1 phase. The results show that the $Mg_{70}Zn_{28}Nd_2$ alloy is in the three-phase region of Mg + Liquid + T_1 at 400 °C.

Fig. 8a is the equilibrium microstructure of $Mg_{70}Zn_{26}Nd_4$ alloy at 400 °C. The black is Mg solid solution with the composition of 98.8% Mg, 1.2% Zn and ignored Nd. According to the results of com-

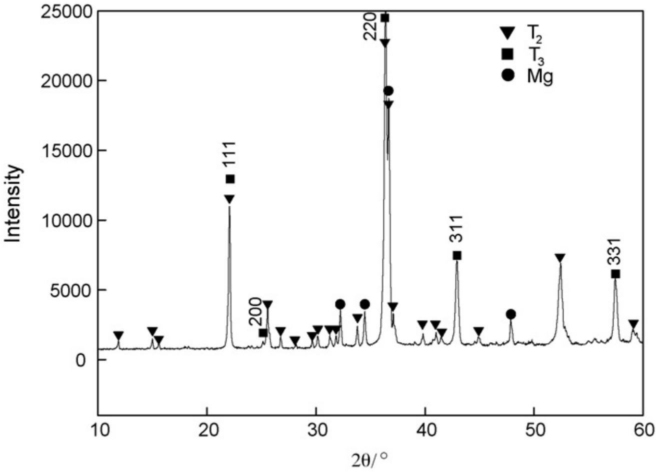

Fig. 5. X-ray diffraction pattern of $Mg_{75}Zn_{17}Nd_8$ alloy at 400 °C.

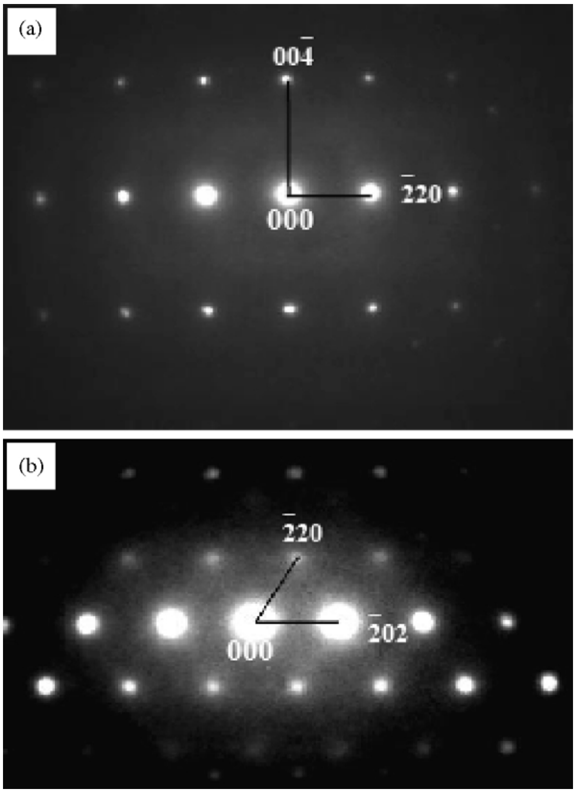

Fig. 6. SAED patterns of T_3 phase in $Mg_{75}Zn_{17}Nd_8$ alloy at 400 °C. (a) [1 1 0] zone axis and (b) [1 1 1] zone axis.

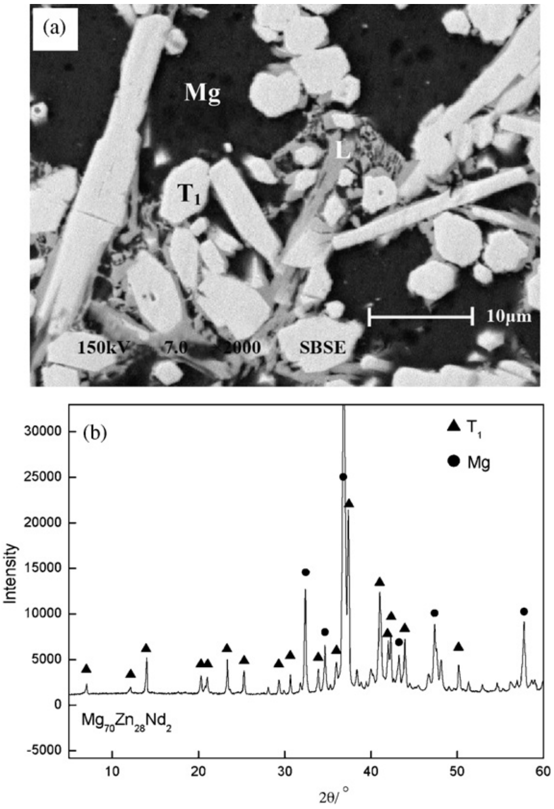

Fig. 7. Microstructure and XRD pattern of alloy $Mg_{70}Zn_{28}Nd_2$ at 400 °C. (a) Microstructure and (b) XRD pattern.

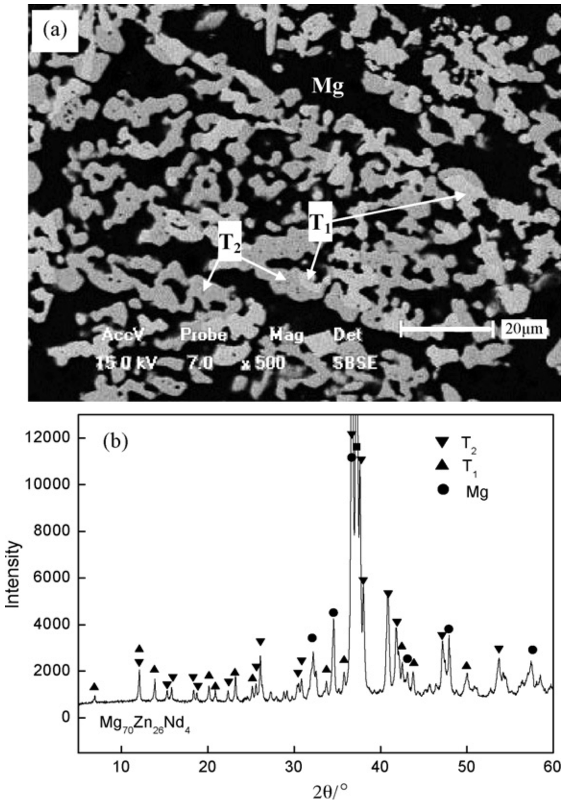

Fig. 8. Microstructure and XRD pattern of $Mg_{70}Zn_{26}Nd_4$ alloy at 400 °C. (a) Microstructure and (b) XRD pattern.

position (Table 1) and the X-ray diffraction pattern (Fig. 8b), the grey must be T_2 phase. The composition of the white is 29.9% Mg, 63.0% Zn and 7.1% Nd, which is the same as that of T_1 phase. As shown in the corresponding X-ray diffraction pattern (Fig. 8b), the characteristic peaks of T_1 phase, T_2 phase and Mg can be indexed. The parameters of T_2 phase in $Mg_{70}Zn_{26}Nd_4$ alloy are $a = 0.965$ nm, $b = 1.118$ nm, and $c = 0.946$ nm. The analysis above shows that the $Mg_{70}Zn_{26}Nd_4$ alloy is in the three-phase region of $Mg + T_2 + T_1$ at 400°C.

3.4. The three-phase equilibrium of $T_2 + T_3 + T_4$

Fig. 9 shows the equilibrium microstructures of $Mg_{51}Zn_{38}Nd_{11}$ alloy and $Mg_{50}Zn_{40}Nd_{10}$ alloy at 400 °C respectively. The characteristic diffraction peaks of T_2 phase and T_3 phase can be indexed in the corresponding X-ray diffraction patterns. The composition of the dark grey matrix is 58.6% Mg, 33.5% Zn and 7.9% Nd, suggesting it is T_2 phase. The bright contains 26.0% Mg, 49% Zn and 25.0% Nd, called T_3 phase. The composition of grey block is 25.4% Mg, 61.0% Zn and 13.6% Nd, and there has no known phase corresponding to it, so that the grey is designated here as T_4 phase. The lattice parameters of T_2 in the two alloys are $a = 0.977$ nm, $b = 1.127$ nm, and $c = 0.956$ nm, and that of T_3 are $a = 0.68$ nm. But the crystal structure of T_4 phase needs to be identified further.

The results reveal that there exists a three-phase region of $T_2 + T_3 + T_4$ in the Mg–Zn–Nd ternary system at 400 °C.

3.5. The partial isothermal section of Mg–Zn–Nd system at 400 °C

The partial isothermal section of phase diagram of Mg–Zn–Nd system at 400 °C (Fig. 10) is deduced from the data discussed all above. It shows clearly that T_2 phase has phase equilibrium with Mg solid solution, T_1 phase, T_3 phase and T_4 phase at 400 °C.

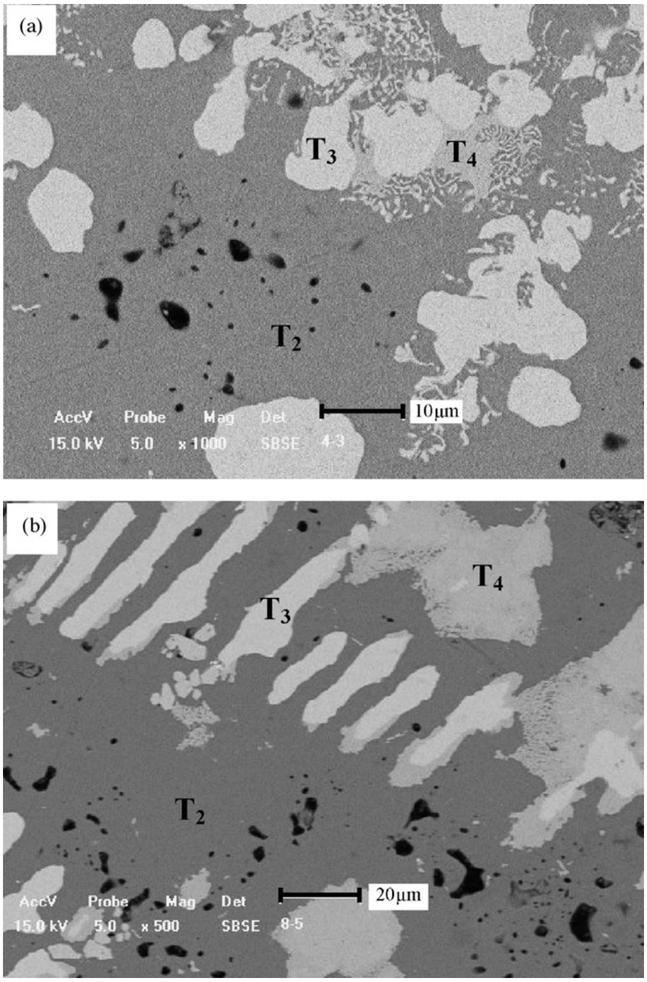

Fig. 9. Microstructures of $T_2 + T_3 + T_4$ three-phase equilibrium alloys at 400 °C. (a) $Mg_{51}Zn_{38}Nd_{11}$ alloy and (b) $Mg_{50}Zn_{40}Nd_{10}$ alloy.

Five three-phase regions and one two-phase region such as $T_2 + T_3 + Mg$, $T_2 + T_1 + Mg$, $T_2 + T_3 + T_4$, $T_2 + T_1 + T_4$, $Mg + T_1 + L$ and $Mg + T_2$ have been identified, and the phase equilibrium of $T_2 + T_1 + T_4$ is deduced by phase equilibrium theory and the experimental results. In addition, the three-phase region of $Mg + T_1 + L$ is matching with the three-phase region of $L + T_1 + Mg_2Zn_3$ reported before [27], and it is also matching with the two-phase region of $Mg + T_2$ obtained in this work.

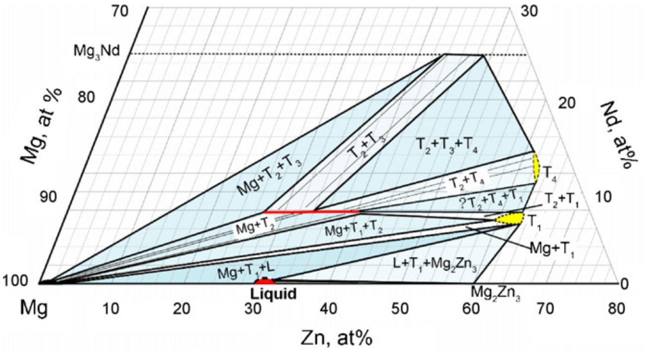

Fig. 10. The partial isothermal section of Mg–Zn–Nd system at 400 °C.

4. Conclusions

1. A ternary linear compound T_2 exists in the low-Nd side of Mg–Zn–Nd system with a chemical formula of $(Mg, Zn)_{11.5}Nd$. Zn content of T_2 is in the range from 26.9% to 41.3%. The crystal structure of T_2 is C-centered orthorhombic with the parameters of $a = 0.965–0.984$ nm, $b = 1.118–1.135$ nm, and $c = 0.946–0.963$ nm.
2. The chemical formula of T_3 phase is $(Mg, Zn)_3Nd$, and the range of Zn content is from 43% to 49%. The crystal structure of T_3 is face-centered cubic with the parameters of $a = b = c = 0.68$ nm.
3. There are five three-phase regions of $T_2 + T_3 + Mg$, $T_2 + T_1 + Mg$, $T_2 + T_3 + T_4$, $T_2 + T_1 + T_4$, $Mg + T_1 + L$ and a two-phase region of $Mg + T_2$ in the isothermal section of Mg–Zn–Nd system at 400 °C.

Acknowledgements

This work is financially supported by National Natural Science Foundation of China under No. 50471025 and National Natural Science Foundation of Liaoning province under No. 20052028.

References

[1] I.B. Bondarev, A.M. Bessonov, Tsvetn. Met. 5–6 (2005) 131–134.
[2] S. Schumann, H. Friedrich, Mater. Sci. Forum 419–422 (2003) 1–56.
[3] C.F. Fang, X.G. Zhang, Y.H. Yu, J.Z. Jin, Heat Treat. Met. 31 (2006) 12–16.
[4] D.J. Li, X.Q. Zeng, J. Dong, C.Q. Zhai, W.J. Ding, J. Alloys Compd. 468 (2009) 164–169.
[5] L.N. Yu, K. Nakata, J.S. Liao, J. Alloys Compd. 480 (2009) 340–346.
[6] M. Eddahbi, P. Perez, M.A. Monge, G. Garces, R. Pareja, P. Adeva, J. Alloys Compd. 473 (2009) 79–86.
[7] Y. Zhao, Y. Gao, D.D. Yin, Q.D. Wang, J.H. Gu, Y. Tong, J. Alloys Compd. 477 (2009) 374–378.
[8] X. Tian, L.M. Wang, J.L. Wang, Y.B. Liu, J. An, Z.Y. Cao, J. Alloys Compd. 465 (2008) 412–416.
[9] W.L. Xiao, S.S. Jia, L.D. Wang, Y.M. Wu, L.M. Wang, J. Alloys Compd. 480 (2009) 33–36.
[10] H.Y. Wu, Z.W. Gao, J.Y. Lin, C.H. Chiu, J. Alloys Compd. 474 (2009) 158–163.
[11] W.L. Xiao, S.S. Jia, J. Wang, J.L. Wang, L.M. Wang, J. Alloys Compd. 458 (2008) 178–183.
[12] C.P. Wang, X. Chen, X.J. Liu, F.S. Pan, K. Ishida, J. Alloys Compd. 458 (2008) 166–173.
[13] P. Bakke, H. Westengen, Magnesium Technology 2005, Metals and Materials Society, Warrendale, 2005, pp. 291–296.
[14] G. Omori, S. Matsuo, H. Asada, Trans. Jpn. Inst. Met. 16 (1975) 247–255.
[15] K. Yu, W.X. Li, R.C. Wang, J. Central South Univ. Technol. 12 (2005) 499–502.
[16] L.Y. Wei, G.L. Dunlop, H. Westengen, Metall. Mater. Trans. 26A (1995) 1705–1716.
[17] J.H. Jun, B.K. Park, J.M. Kim, K. Kim, W.J. Ung, Mater. Sci. Forum 510–511 (2006) 214–217.
[18] T. Wada, T. Shinkawa, S. Kamado, Y. Kojima, J. Jpn. Inst. Light Met. 45 (1995) 504–509.
[19] Q. Li, Q.D. Wang, Y.X. Wang, X.Q. Zeng, W.J. Ding, J. Alloys Compd. 427 (2007) 115–123.
[20] W.J. Ding, D.Q. Li, Q.D. Wang, Q. Li, Mater. Sci. Eng. 483–484 A (2008) 228–230.
[21] J. Yang, J.L. Wang, L.D. Wang, Y.M. Wu, L.M. Wang, H.J. Zhang, Mater. Sci. Eng. 479A (2008) 339–344.
[22] J.S. Zhang, J. Yan, W. Liang, E.L. Du, C.X. Xu, J. Non-Cryst. Solids 355 (2009) 836–839.
[23] J.S. Zhang, J. Yan, W. Liang, C.X. Xu, C.L. Zhou, Mater. Lett. 62 (2008) 4489–4491.
[24] M.E. Drits, E.M. Padezhnova, N.V. Miklina, Russ. Metall. 3 (1974) 143–146.
[25] V.V. Kinzhibalo, A.T. Tyvanchuk, E.V. Melnik, Stable and Metastable Phase Equilibria in Metallic Systems, Nauka, Moscow, USSR, 1985, pp.70–74.
[26] P. Villars, A. Prince, H. Okamoto, Handbook of Ternary Alloy Phase Diagrams CD-ROM, ASM International, Ohio, 1997.
[27] M.L. Huang, H.X. Li, J.Y. Yang, Y.P. Ren, H. Ding, S.M. Hao, Acta Metall. Sin. 44 (2008) 385–390.